Indian Journal of Chemical Technology
Vol. 31, May 2024, pp. 462-469
DOI: 10.56042/ijct.v31i3.4983

Synthesis and characterization of ZnO/activated carbon khat nanocomposite for removal of methylene blue dye

Bantie Yasabu Mekonnen[1]*, Dessale Alemu Fentaw[2] & Moges Abebe Zeleke[1]

[1]Department of Chemistry, Woldia University, Woldia, Ethiopia
[2]Department of Physics, Woldia University, Woldia, Ethiopia

*E-mail: bantieyas09@gmail.com

Received 18 August 2023; accepted 23 February 2024

The rapid expansion of textile industries causes a massive release of dyes to the water bodies. The primary source of water pollution is this huge rise in dye use, which has a negative impact on aquatic life and equilibrium of the ecosystem. The purpose of the present study is the synthesis and characterization of a composite material namely zinc oxide incorporated activated carbon khat for effective adsorption of methylene blue dye. Fourier transforms infrared spectroscopy, UV-Visible spectroscopy and Brunaeur, Emmett and Teller surface area analysis studies have been used to characterize the composite. Experimental conditions such as contact time, adsorbent dosage, concentration of the dye solution, solution temperature and solution pH have been altered to find out the optimum conditions of adsorption. The optimum pH has been found to be 8.0 and dosage of composite has been optimized as 0.3 g for a dye concentration of 20 ppm and equilibrium was attained at 60 min. The adsorption kinetics of the adsorbent revealed that pseudo-second-order kinetic model is better fitted with a good correlation coefficient, and the equilibrium data fitted well with the Freundlich isotherm model.

Keywords: Dye removal, Isotherm, Kinetic model, Methylene blue removal, ZnO/activated carbon khat nanocomposite

Introduction

Nowadays the advancement of science and technology coupled with rapid growth of the global population, urbanization and industrialization has a great influence on water pollution[1-3]. Globally water pollution caused by mainly the discharge of industrial effluents, human activities and natural processes is the major issue and concern[4–8]. Organic and inorganic contaminants from industries infiltrate into water bodies significantly affected water quality, resulting in an increasing freshwater crisis worldwide[3,9]. The disposal of industrial effluents has become major issue [10-13] and their removal/ treatment before directly discharge into water bodies are an environmental concern and utmost area of research because they are not only pollute water but also disrepute the aquatic ecosystem. Although textile industries have been a major contributor to the world economy, pollution level from dyes is increasing[14] and maintainability issues should be considered at each point of the source level. Dyes transform into dangerous pollutants when they are improperly handled and disposed of causing serious environmental and public health hazards[12,15].

Methylene blue (MB) is one of the most frequently used basic dyes in several applications including dyeing of cotton, leather, wool, paper, silk and the production of ink and quality control test of concrete and motor [14, 16]. The releasing of this dye into the environment and water bodies can causes various acute and chronic effects to living things including human beings like skin irritation, itching, carcinogenic, diarrhea, vomiting, chest pain severe headache and even can cause a permanent injury to animal eyes[5,9,14]. Removal of MB from wastewater could be achieved by different approaches, including ion-exchange, chemical precipitation, chemical oxidation, flocculation, membrane filtration, reverse osmosis, coagulation, biodegradation, adsorption and photocatalytic degradation[3,9,13,16-19]. Among them adsorption techniques have many advantages due to its cost-effectiveness, simple operational process and high efficiency[20].

In recent years, nanomaterials have been synthesized and applied for efficient removal of dye through photocatalytic activities[2,12,18]. This is due to their unique physicochemical properties such as their structures, high mechanical strength, high width to

height ratio, broad range of radiation absorption and high photo stability. Metal oxide-based compounds such as zinc oxide (ZnO) have attracted a lot of consideration as adsorbent materials due to their high surface area and strong adsorption ability[15]. From metal oxide, ZnO nanoparticles have been reported as an efficient and effective adsorbent in heavy metal and organic dye removal with low cost which makes it economically valuable[1,15] and on the top of this various studies shows that ZnO nanoparticle composite can increase the removal efficiency of metal pollutant and organic dye than ZnO nanoparticle[4, 10].

This study was aimed to synthesise ZnO-activated carbon khat (ACK) composite. The synthesized materials were characterized by analytical instruments such as Fourier transform infrared spectroscopy (FTIR) and UV–visible spectroscopy. The study was dedicated to examining the capability of ZnO-ACK as a low cost adsorbent to remove MB dye from aqueous solutions. The effects of experimental parameters such as initial dye concentration, contact time, solution pH and adsorbent dosage were studied. Adsorption kinetics and isotherm models were carried out on adsorption performance of ZnO-ACK composite.

Experimental Section

Synthesis and carbonization of Khat (*Catha edulis*)

The preparation of activated carbon of Khat was conducted according to the following procedure. To get rid of any dust and other water-soluble contaminants, the sample was cleaned with distilled water. After the stem was exposed to many dyes in the sun, it was oven-dried at 105 °C until it was entirely dry, at which point it was sliced into 10 mm long pieces. Following drying, the material was ground in a ball mill and separated using hand shaking of stainless steel mesh screens with a typical 1 mm sieve opening. After the raw material was sieved, it was carbonized and physically activated in a muffle furnace (Nabertherm B180) for 2 h at 400 °C without air. The sample was kept sealed inside a stainless steel tube. After that, the sample was allowed for few minutes to cool. In order to perform the chemical activation, the necessary weight of powdered material was submerged in 1 N of NaOH for 12 h at a mass ratio of 1:5 w/v. After the sample was soaked, it was filtered using Whatman filter paper, repeatedly rinsed with 2 N HCl, and then distilled water until the pH was neutral. In order to obtain a good carbon structure and a high surface area, the resultant activated carbon was completely dried at 110 °C in an oven for 3 h. It was then stored in desiccators for further analysis[20,21].

Synthesis of ZnO nanoparticle

For ZnO nanoparticle synthesis, a magnetic stirrer was used to heat up a beaker with 20 g of zinc chloride and 100 mL of deionized water to 90 °C, and the mixture was agitated for 45 min. In another beaker, 7.27 g of NaOH was dissolved in 100 mL of deionized water and stirred for 20 min. With steady stirring, 58 mL of a NaOH solution were added to the beaker holding the $ZnCl_2$ solution. The aqueous solution turned into a milky white colloid without any precipitation. Following the full addition of NaOH, the reaction was allowed to run for 2 h. The solution was allowed to settle and then filtered using Whatman filter. The filtered sample was allowed to dry in oven at 160 °C for 7 h, and calcinated at 200°C for 2 h in a muffle furnace. Finally, the material was grinded using mortar and pestle[22].

Synthesis of ZnO nanoparticle loaded with activated carbon khat (ZnO-ACK)

The ZnO nanoparticle-carbonized khat was prepared by adding 10 g of synthesized ZnO nanoparticle into 100 mL distilled water and stirred vigorously on a magnetic stirrer for 30 min. Then, 5 g of activated carbon khat was added into the solution with continuous stirring for 30 min at 100 °C. The obtained product was then filtered and washed several times with double de-ionized water. The filtrate ZnO loaded activated carbon khat was dried in a hot air oven for 4 h at 200 °C and then stored at room temperature for characterization and application.

Adsorption studies

The potential of ZnO-ACK composite as adsorbent for the removal of MB dye from aqueous solution was carried out by batch process. The experiments were conducted in 250 mL of conical flask containing 40 mL of MB and 0.1 g of adsorbents was added into the solution. The mixed solutions were agitated with magnetic stirrer on digital hot plate at 400 rpm. After wards, the adsorbent material was separated from the solution by centrifuging at 8000 rpm for 10 min. Finally, the absorbance of supernatant solution was determined by using UV–visible spectrophotometer at a maximum wave length of 618 nm. The influence of change in pH (2-12), contact time (10-80 min), initial

concentration of adsorbate (10-60 ppm) and the adsorbent dose (0.08-0.8 g) were studied. The equilibrium concentrations of MB removed and the removal percentage were calculated using the following Eqs (1 & 2).

$$q_e \ \frac{mg}{g} = \frac{(C_O - C_1)V}{m} \quad \ldots (1)$$

$$Removal\ efficiency\ (\%) = \frac{C_O - C_1}{C_O} x\ 100 \quad \ldots (2)$$

Where, q_e is the equilibrium concentration of removed MB onto the composite surface (mg/g). C_o and C_1 are initial (mg/L) and equilibrium concentration of MB at equilibrium time (mg/L), respectively. V and m are solution volume (mL) and adsorbent mass (g) respectively.

Results and Discussion

Surface area determination

According to Sear method, the specific surface area of the adsorbent was calculated. 1.5 g of synthesised adsorbent and 30 g of NaCl samples were dissolved with 100 mL of distilled water in 250 mL conical flask. The solution's pH was then brought down to 4, and it was titrated with 0.1 M NaOH until it reached 9. The amounts of NaOH that were needed to adjust the pH from 4 to 9 were noted. The following formula was used to get the sample's precise surface area[21].

$$\text{Specific surface area } (\frac{m2}{g}) = 32v - 25 \quad \ldots (3)$$

Where V is the volume of 0.1 M NaOH required raising the pH from 4.0 to 9.0.

Table 1 displays the precise surface area of synthesised activated carbon based on analysis using the Sear method. Based on this finding, the produced adsorbent may have a relatively high surface area as a result of the activation of sodium hydroxide. When sodium hydroxide is activated at high concentrations, the chemical components are reorganized, which causes carbon-rich molecules to deposit in the biomass voids as a result of temperature and pressure changes that increase the surface area of the adsorbent[19].

Optimization results of different parameters

Effects of solution pH

In adsorption process pH of solution has a significant effect on adsorption efficiency and electrostatic interaction between adsorbent and adsorbate[23-25.] Basicity and alkalinity of solution affects electrical charge of the adsorbent surface and dissociation of different functional groups in active sites of the adsorbent[23]. The basic dyes give positively charged ions when dissolved in water and in acidic medium positively charged surface of sorbent tends to oppose the adsorption of cationic sorbate species. When the pH of dye solution increases, the surface tends to acquire negative charge, there by resulting in an increased adsorption of dyes due to increasing electrostatic attraction between positively charged sorbate and negatively charged sorbent[24]. MB dye is an aromatic heterocyclic basic dye [25] having a molecular weight of 319.85 g mol^{-1}. A literature shows the removal of MB dye increase as pH of solution increases due to good electrostatic attraction between the dye and adsorbent. As shown in Fig. 1 removal efficiency of MB with synthesized ZnO-ACK composite nanoparticle increases as pH changes from 2-8 and decrease from pH value 8-12. This is due to basic nature of MB dye and as the pH increases and becomes more alkaline, the dye molecules tend to become partially or fully deprotonated, resulting in a decrease in their positive charge. This reduces the

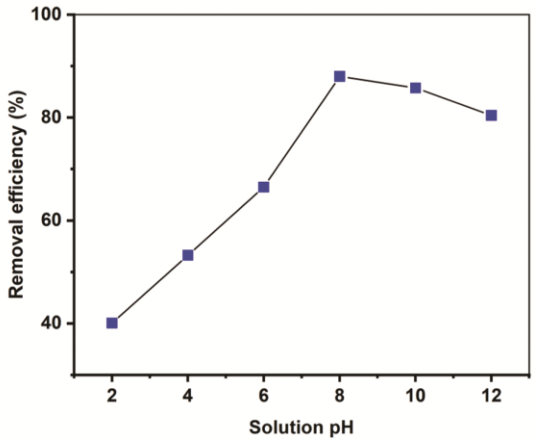

Fig. 1 — Effect of solution pH on the removal of MB dye

Table 1 — Kinetics parameters obtained from the graph

Kinetic model	q_e experimental	q_e calculated	K	R^2
Pseudo 1st	15.2060	9.9531	-0.00858	0.9236
Pseudo 2nd		18.1455	0.00246	0.9699
Interparticle diffusion			1.52576	0.92386

attraction between the dye molecules and the negatively charged adsorbent surface, leading to a decrease in the adsorption capacity[24].

Effects of adsorbent dose

The adsorbent active site available for pollutant adsorption depends on amount of adsorbent dose and the removal efficiency depends on it[26]. The effect of adsorbent dose on the percent removal of MB dye at various concentrations of ZnO-ACK composite (0.1, 0.2, 0.3, 0.4, 0.5 and 0.6 g) is shown in Fig. 2. The removal efficiency of ZnO-ACK composite increase as its mass increased from 0.1-0.3g and decrease as its mass increase from 0.4-0.6g. The removal efficiencies increased when the amount of ZnO-ACK composite increased, as the number of the active sites to which the dye molecules could bind increased. Due to the limited available surface area and the increased diffusion resistance, overall adsorption capacity might be decreased[26].

Effect of contact time

To determine the time dependence of the adsorption of MB dye, time was varied between 10 and 70 min. Removal percentage of MB from the solution by adding fixed amount of adsorbent was measured by UV-visible spectrophotometer at different contact time starting from 10 to 70 min shown in Fig. 3. At various contact time for dye removal treatment with shaking, the impact of the period of shaking observed as the optimum dye removing percentage was found to be 82% at 60 min.

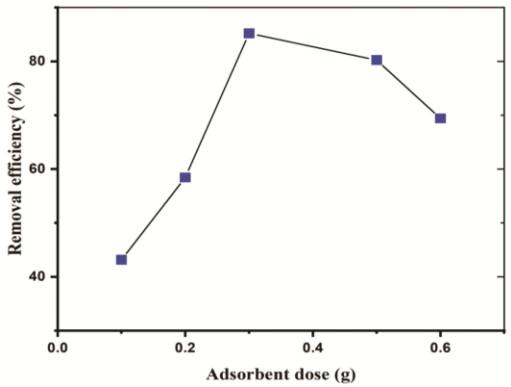

Fig. 2 — Effect of adsorbent dose on the removal of MB dye

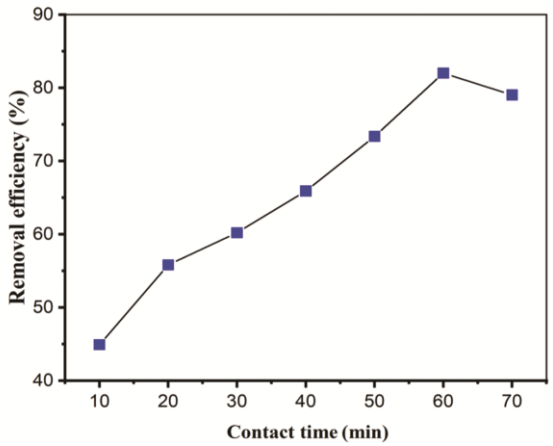

Fig. 3 — Effect of contact time on the removal of MB

Effect of dye concentration

The initial dye concentration affects dye removal efficiency of the adsornents[19]. The effect of initial concentration of MB is shown in Fig. 4. When initial dye concentrations were increased from 10 ppm to 60 ppm, the dye removal efficiency result indicates: 10 ppm (70.37%), 20 ppm (84.53 %), 30 ppm (81.23 %), 40 ppm (77.35 %), 50 ppm (71.94%) and 60 ppm (64.56%). The maximum MB dye removal efficiency (84.53 %) is at concentration of 20 ppm and decrease as concentration increase to 60 ppm (64.56%). The percentage of MB dye removal result agrees with the previously reported results by other researchers[19]. Initially increase from 70.37% at 10 ppm to 84.53% at 20 ppm may be due to high driving force of mass transfer of dye and removal efficiency decreases with increasing initial dye concentration, which leads to a saturation of adsorption sites on the adsorbent surface.

Effect of temperature

The effect of temperature on adsorption of MB dye on ZnO-ACK composite was examined from 25 ℃ to 65 ℃. As shown from Fig. 5 the removal efficiency of the adsorbent increase from 25 ℃ to 35 ℃ and after 35 ℃, the removal efficiency found to be almost constant. At high temperature, the adsorption capacity of the adsorbent in this study found to be decreased

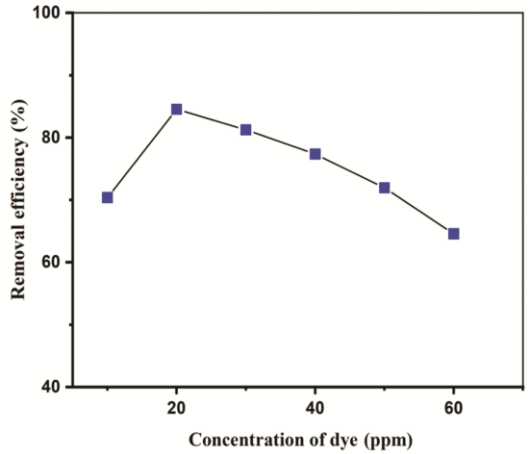

Fig. 4 — Effect of initial concentration of MB dye on removal efficiency

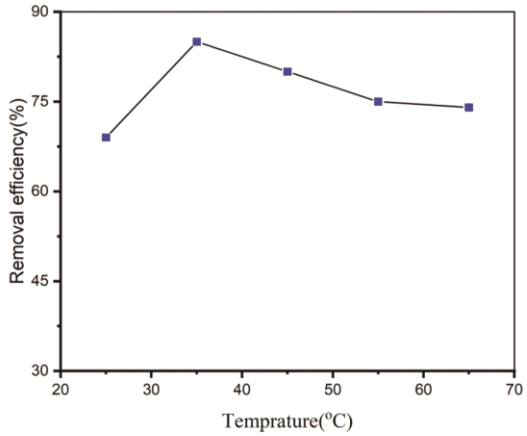

Fig. 5 — Effect of temperature on removal efficiency

this confirmed that the thermodynamics process is exothermic[11]. The optimum and favourable adsorption process is obtained at a low temperature which is at 35 ℃. Additionally, the dye is more soluble, and the interaction between the solute and the solvent is higher than the interaction between the solute and the adsorbent, making solute adsorption more difficult.

Kinetic studies

Chemical kinetics research involves keeping a close eye on the experimental circumstances since they might affect how quickly a chemical reaction proceeds and how quickly equilibrium is reached. The validity of many kinetic models, including pseudo-first-order (Eq. 4), pseudo-second-order (Eq. 5), and intra-particle diffusion (Eq. 6), with respect to the experimental adsorption data for MB has been tested in this study.

$$log(qe - qt) = log\ qe\ - K_1 t \quad \ldots (4)$$

$$\frac{t}{qt} = \frac{t}{qe} + \frac{1}{K_2 qe 2} \quad \ldots (5)$$

$$qt = K_{diff}\, t^{1/2} + C \quad \ldots (6)$$

Where q_e (mg/g) is the amount adsorbed at equilibrium time; q_t (mg/g) is the amount adsorbed at a time, t (min); K_1 is the pseudo-first-order rate constant (Fig. 6); K_2 is the pseudo-second-order rate constant (Fig. 7); k_{diff} (mg/g $min^{1/2}$) is the intra-particle diffusion rate constant (Fig. 8), and C is the intercept that indicates the boundary layer thickness. The kinetic rate constant, k, and q_e for each model can be calculated by plotting graph log ($q_e - q_t$) versus t for pseudo-first-order, t/q_t versus t for pseudo-second-order models, and q_t versus $t_{1/2}$ for intra-particle diffusion models and the graphs as shown in Figs 6-8.

As shown in Table 1 the calculated amount of dye adsorbed through pseudo second order is

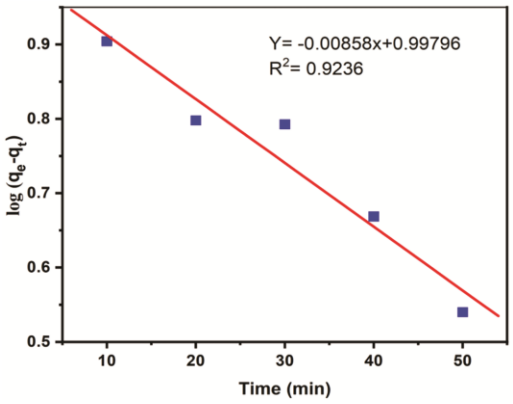

Fig. 6 — Plot for pseudo 1st order reaction model

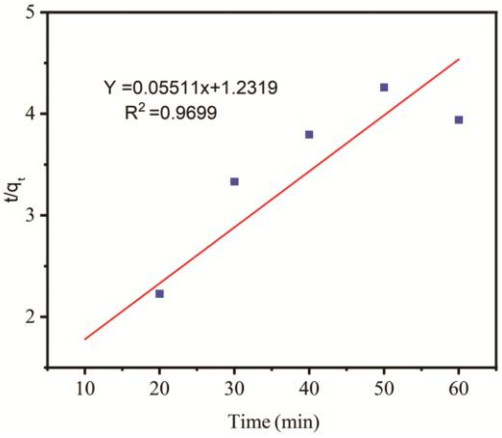

Fig. 7 — Plot for pseudo 2nd order reaction model

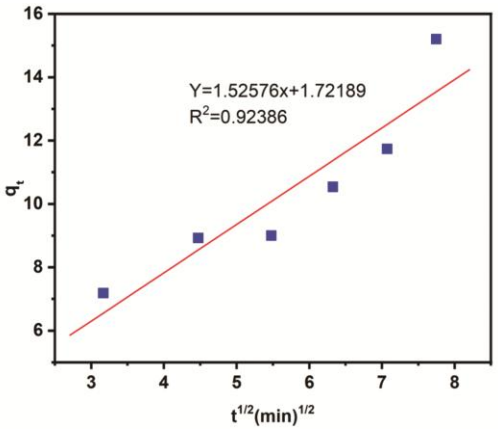

Fig. 8 — Plot for Inter-particle diffusion model

approximately equal to experimentally obtained value and the value of correlation coefficient of pseudo second order (R^2=0.9699) is greater than that of both pseudo first order (R^2= 0.923) and Inter-particle diffusion model (R^2 =0.92386) . This result showed that the adsorption process of MB on as synthesized nanocomposite follows pseudo second order model.

Sorption Isotherms

In the present study, two isotherm equations, namely Langmuir and Freundlich were used for the analysis of the isotherm data. The equation for Langmuir isotherm is represented as follows.

$$\frac{Ce}{qe} = \frac{1}{qem} + \frac{Ce}{qm} \quad \ldots (7)$$

Where C_e is the equilibrium concentration of MB (mg/L), q_e is the quantity of MB dye adsorbed at equilibrium (mg/g), q_{max} is the maximum amount of MB sorbet (mg/g), and b is the desorption constant (L/mg). A plot of $1/C_e$ versus $1/q_e$ gives a linear plot, and q_{max} and b can be obtained from the intercept and slope of the plot, respectively.

The linear expression of the Freundlich isotherm model can be illustrated in

$$\log q_e = \log K_f + \frac{\log Ce}{n} \quad \ldots (8)$$

where q_e represents the equilibrium amount of MB dye adsorbed by the adsorbent, (mg/g), K_f represents the Freundlich constant that shows adsorption capacity (mg/L), *n* represents the intensity of the adsorption constant, and C_e represents the equilibrium concentration of MB dye solution (mg/L)[27]. The parameters of Freundlich isotherms can be obtained from a linear plot of log q_e versus log C_e (Fig. 9). K_f can be calculated from the intercept of the linear plot and n can be obtained from the slope of the equation and if its value is greater than one (n>1) the adsorption system would be favoured [11].

The correlation coefficients of Freundlich (R^2 =0.8823) is provides a fitted model for the sorption system than the Langmuir model (R^2=0.73729).The maximum monolayer adsorption capacity of MB was found to be 59.98 mg/g from the Langmuir isotherm model equation (Fig. 10). The maximum removal for this study is greater than the removal efficiency of cress seed mucilage with magnetic iron oxide nanoparticles (44.6 mg/g) and Cotton Rope Coated with Cyclodextrin Polymers (23.7 mg/g) for removal of MB dyes from aqueous solution reported by [5,28] respectively.

In addition to this, the feasibility of the adsorption system at different initial dye concentrations was examined by using a dimensionless constant separation factor (RL) and the value of RL for each initial dye concentration can be determined by

$$RL = \frac{1}{1+bCo} \quad \ldots (9)$$

Where RL represents the separation factor, b represents the Langmuir constant (L/mg), and CO represents the initial concentration of MB dye (mg/L)[18]. RL > 1 implies an unfavourable monolayer adsorption process and RL=1 indicates a linear process. The process is favourable when 0 < RL < 1 and irreversible when RL= 0. In this study the value of RL at all dye concentration is less than unity, which confirmed the favourable adsorption of MB dye over the adsorbent[21].

FTIR analysis

Synthesized ZnO nanoparticles and ZnO-ACK composites were subjected to FT-IR analysis to detect the various characteristic functional group associated with the synthesized nanoparticles and composite. FTIR spectrum of the synthesized nanoparticles and composite showed in Fig. 11. All the observed peaks were compared from previous literatures in order to confirm the findings. Similar findings were also found from previous studies related to ZnO NPs synthesis and characterization[29, 32, 33]. Absorption spectra for metal oxides their band arise below 1000 cm^{-1} due to

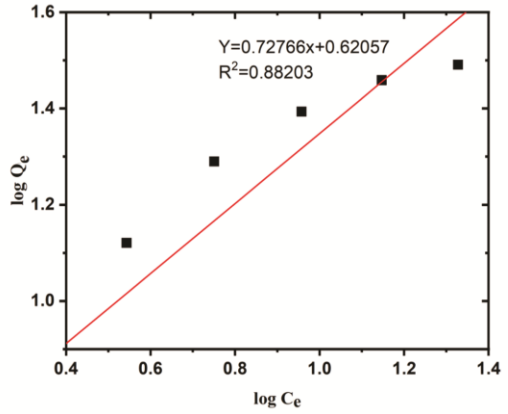

Fig. 9 — Plot for Freundlich isotherm model

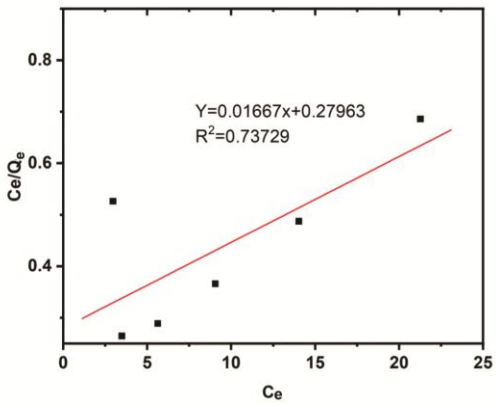

Fig. 10 — Plot for Langmuir isotherm model

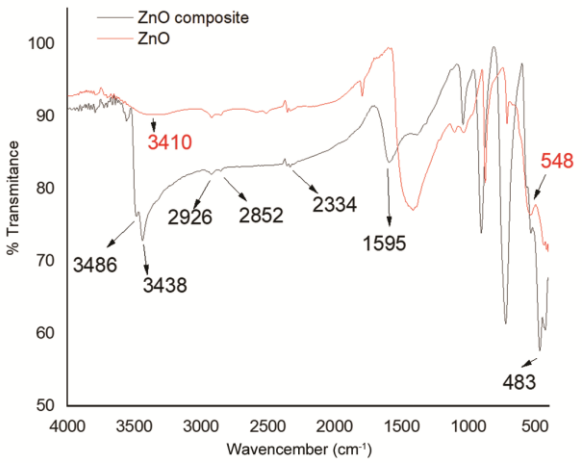

Fig. 11 — FTIR spectra of ZnO nanoparticles and ZnO-ACK composite

inter-atomic vibrations[34]. For the synthesized ZnO nanoparticles, FTIR spectrum shows weak broad band at 3410 cm^{-1}may be due to O–H stretching of water[31,33,35]. The absorption peak at 548cm^{-1} corresponds to Zn-O bond stretching fitted with reported value [22].

The FT-IR spectrum for activated carbon of khat is used from literature [21] for comparison. As indicated from the reference [21]; the broad peak at 3440 cm^{-1} appears due to O–H stretching of hydroxyl group. A pair of peaks at 2920 and 2840 cm^{-1} could be attributed to sp^3 C–H stretching. The peak at the interval between 2345 - 2450 cm^{-1} is may be due to sp carbon to carbon stretching vibrations of alkyne, the band between 1500– 1700 cm^{-1} may be due to C=C and C=O stretching frequency of aromatic hydrocarbons, aldehyde or ketone, the band attributed between 1250– 1000 cm^{-1} is assigned to C–O vibration of carboxylic acids, C–O–C and O–H vibration of polysaccharides, 1000–500 cm^{-1} band interval is assigned to C–H and C–C bend vibration.

FTIR spectra of ZnO-ACK composite shows peak shift from ZnO nanoparticles and activated carbon of khat due to change in electronic environment of free metal oxide nanoparticles and activated carbon of khat. A pair of peaks at 3486 and 3438 cm^{-1} indicates there is N-H stretching of amide or amine of activated carbon of khat[35], sp^3 C-H stretching shifts to higher wave number relatively from ZnO and activated carbon of khat due to a change in the electronic environment due to composite formation of ZnO with activated carbon of khat. The peak at 2334 cm^{-1} in the composite is due to the presence of C≡C triple bond of alkyne and 1595-1338 cm^{-1} indicates the presence of C=C or C=O double bond from activated carbons of khat. The peak at 483 cm^{-1} may be attributed due to Zn-O bond stretching frequency.

Conclusion

The present investigation showed that ZnO-ACK composite was an effective adsorbent for removal MB from aqueous solution. Experimental processes were carried out as a function of parameters like solution pH, initial dye concentrations, contact time, adsorbent dosage and temperature. The kinetics study of MB adsorption on ZnO-ACK composite material was tested with three models like pseudo-first-order, pseudo-second-order model and Inter-particle diffusion model. The high value of correlation coefficient of pseudo-second-order model revealed that the adsorption kinetics agreed well with this model. Adsorption equilibrium data examined on Langmuir and Freundlich models and equilibrium data fitted very well in Freundlich isotherm equations. The maximum MB adsorption of the adsorbent was found to be 59.98 mg/g. The present study confirmed that the prepared composite was effective adsorbent for the removal of MB dyes from aqueous solutions.

References

1 Chakraborty S, Farida J J, Simon R, Kasthuri S & Mary N L, *Averrhoe carambola* fruit extract assisted green synthesis of zno nanoparticles for the photodegradation of congo red dye, *Surf Interfaces*, 19 (2020) 1.

2 Roy1 A, Murthy A H, Ahmed H M, Islam M N & Prasad R, Review on phytogenic synthesis of metal/metal oxide nanoparticles for degradation of dyes, *J Renew Mater*, 10 (2022) 1911.

3 Al-Mur B A, Green zinc oxide (ZnO) nanoparticle synthesis using mangrove leaf extract from avicenna marina: Properties and application for the removal of toxic metal ions (Cd^{2+} and Pb^{2+}), *Water*, 15 (2023) 1.

4 Oyewo O A, Adeniyi A, Sithole B B & Onyango M S, Sawdust-based cellulose nanocrystals incorporated with ZnO nanoparticles as efficient adsorption media in the removal of methylene blue dye, *Am Chem Soc*, 5 (2020) 18798.

5 Allafchian A, Mousavi Z S & Hosseini S S, Application of cress seed musilage magnetic nanocomposites for removal of methylene blue dye from water, *Int J Biol Macromol*, 136 (2019) 199.

6 Taymaz1 B H, Kamiş H & Yoldaş O, Photocatalytic degradation of malachite green dye using zero valent iron doped polypyrrole, *Korean Soc Environ Eng*, 27 (2022) 1.

7 Bhatia P & Nath M, Green synthesis of p-NiO/n-ZnO nanocomposites: Excellent adsorbent for removal of congo red and efficient catalyst for reduction of 4-nitrophenol present in wastewater, *J Water Process Eng*, 33 (2020) 1.

8 Taha A, Da'na E & Hassanin H A, Modified activated carbon loaded with bio-synthesized Ag/ZnO nanocomposite and its application for the removal of Cr (VI) ions from aqueous solution, *Surf Interfaces*, 23 (2021) 1.

9 Dutta S, Gupta B, Srivastava S K & Gupta A K, Recent advances on the removal of dyes from wastewater using various adsorbents: A critical review, *Royal Soc Chem*, 2 (2021) 4497.

10 Modi S & Fulekar M H, Synthesis and characterization of zinc oxide nanoparticles and zinc oxide/cellulose nanocrystals nanocomposite for photocatalytic degradation of methylene blue dye under solar light irradiation, *Environ Eng Nanotechnol*, 18 (2020) 1.

11 Mekonnen B Y, Abate G Y, Mekonnen S D & Gebeyehu A G, Adsorption of methylene blue dye onto acid-treated tej residue: Kinetic, equilibrium and thermodynamic study, *Indian J Chem Technol*, 30 (2023) 94.

12 Fouda A, Salem S S, Wassel A R, Hamza M F & Shaheen T I, Optimization of green biosynthesized visible light active CuO/ZnO nano-photocatalysts for the degradation of organic methylene blue dye, *Heliyon*, 6 (2020) 1.

13 Shimi A K, Parvathiraj C, Kumari S, Dalal J, Kumar V, Wabaidurd S M & Alothman A Z, Green synthesis of SrO nanoparticles using leaf extract of *Albizia julibrissin* and its recyclable photocatalytic activity: An eco-friendly approach for treatment of industrial wastewater, *Royal Soc Chem*, 1 (2022) 849.

14 Kamaraj M, Srinivasan N R, Assefa G, Adugna A T & Kebede M, Facile development of sunlit ZnO nanoparticles-activated carbon hybrid from pernicious weed as an operative nano-adsorbent for removal of methylene blue and chromium from aqueous solution: Extended application in tannery industrial wastewater, *Environ Technol Innov*, 17 (2020) 1.

15 Joicy A A, Selvamani R, Janani C, Balasubramanian C, Prabhu K, Marimuthu K, Bupesh G, Vijayakumar T S & Saravanan K M, Photocatalytic degradation of textile dye using green synthesized nanoparticles, *Nanobioscince*, 12 (2023) 1.

16 Kara H T, Anshebo S T, Sabir F K & Workineh G A, Removal of methylene blue dye from wastewater using periodiated modified nanocellulose, *Int J Chem Eng*, 2021 (2021) 1.

17 Moosavi S, Man R Y, Lai C W, Yusof Y, Gan S, Akbarzadeh O, Chowhury Z Z, Yue X G & Johan M R, Methylene blue dye photocatalytic degradation over synthesised Fe_3O_4/AC/TiO_2 nano-catalyst: Degradation and reusability studies, *Nanomaterials*, 10 (2020) 1.

18 Elbadawy H A, Elhusseiny A F, Hussein S M & Sadik W A, Sustainable and energy-efficient photocatalytic degradation of textile dye assisted by ecofriendly synthesized silver nanoparticles, *Sci Reports*, 13 (2023) 4497.

19 Soltani A, Faramarzib M & Parsa S A, A review on adsorbent parameters for removal of dye products from industrial wastewater, *Water Qual Res J*, 56 (2021) 181.

20 Alswat A A, Ashmali A M, Alqasmi T M, Alhassani H R & Alshorif F T, Role of nanohybrid NiO–Fe_3O_4 in enhancing the adsorptive performance of activated carbon synthesized from yemeni-khat leave in removal of Pb (II) and Hg (II) from aquatic systems, *Heliyon*, 9 (2023) 1.

21 Abate G Y, Alene A N, Habte A T & Getahun D M, Adsorptive removal of malachite green dye from aqueous solution onto activated carbon of catha edulis stem as a low cost bio-adsorbent, *Environ Syst Res*, 9 (2020) 1.

22 Zhou X Q, Hayat Z, Zhang D D, Li M Y, Hu S, Wu Q, Cao Y F & Yuan Y, Zinc oxide nanoparticles: Synthesis, characterization, modification and applications in food and agriculture, *Processes*, 11 (2023) 1193.

23 Mousavi S A, Mahmoudi A, Amiri S, Darvishi P & Noori E, Methylene blue removal using grape leaves waste: Optimization and modeling, *Appl Water Sci*, 12 (2022) 1.

24 Boumediene M, Benaïssa H, George B, Molina S & Merlin A, Effects of pH and ionic strength on methylene blue removal from synthetic aqueous solutions by sorption onto orange peel and desorption study, *J Mater Environ Sci*, 9 (2018) 1700.

25 Khan I, Saeed K, Zekker I, Zhang B, Hendi A H, Ahmad A, Ahmad S, Zada N, Ahmad H, Shah L A, Shah T & Khan I, Review on methylene blue: Its properties uses, toxicity and photodegradation, *Water*, 14 (2022) 1.

26 Ortíz A V, Lopez K F & Toro R O, Kinetics and adsorption equilibrium in the removal of azo-anionic dyes by modified cellulose, *Sustainability*, 14 (2022) 1.

27 Edokpayi J N, Alayande S O, Adetoro A & Odiyo J O, The equilibrium, kinetics, and thermodynamics studies of the sorption of methylene blue from aqueous solution using pulverized raw macadamia nut shells, *J Anal Methods Chem*, 2020 (2020) 1.

28 Martwong E, Sukhawipat N & Junthip J, Adsorption of cationic pollutants from water by cotton rope coated with cyclodextrin polymers, *Polymers*, 14 (2022) 2312.

29 Shamhari N M, Wee B S, Chin S F & Kok K Y, Synthesis and characterization of zinc oxide nanoparticles with small particle size distribution, *Acta Chim Slov*, 65 (2018) 578.

30 Elhamdi I, Souissi H, Taktak O, Elghoul J, Kammoun S, Dhahri E & Costa B F, Experimental and modeling study of ZnO: Ni nanoparticles for near-infrared light emitting diodes, *Royal Soc Chem*, 12 (2022) 13074.

31 Peres M L, Delucis R A, Amico S C & Gatto D A, Zinc oxide nanoparticles from microwave-assisted solvothermal process: Photocatalytic performance and use for wood protection against xylophagous fungus, *Nanomater Nanotechnol*, 9 (2019) 1.

32 Khan M, Naqvi A H & Ahmad M, Comparative study of the cytotoxic and genotoxic potentials of zinc oxide and titanium dioxide nanoparticles, *Toxicol Rep*, 2 (2015) 765.

33 Bekele B, Jule L T & Saka A, The effects of annealing temperature on size, shape, structure and optical properties of synthesized zinc oxide nanoparticles by sol-gel methods, *Dig J Nanomater Biostruct*, 16 (2021) 471.

34 Priyadharsini N, Bhuvaneswari N & Joshy J, Plant mediated synthesis of ZnO and Mn doped ZnO nanoparticles using carica papaya leaf extract for antibacterial applications, *Asian J Appl Sci Technol*, 5 (2021) 69.

35 Aklilu M & Aderaw T, Khat (*Catha edulis*) leaf extract-based zinc oxide nanoparticles and evaluation of their antibacterial activity, *J Nanomater*, 2022 (2022) 1.

36 Mittal H, Babu R, Dabbawala A A & Alhassan S M, Low-temperature synthesis of magnetic carbonaceous materials coated with nanosilica for rapid adsorption of methylene blue, *Am Chem Soc*, 5 (2020) 6100.

37 Djilani C, Zaghdoudi R, Djazi F, Bouchekima B, Lallame A, Modarressif A & Rogalski M, Adsorption of dyes on activated carbon prepared from apricot stones and commercial activated carbon, *J Taiwan Institute of Chem Eng*, 53 (2015) 112.